MARITIME TRANSPORTATION RESEARCH AND EDUCATION CENTER
TIER 1 UNIVERSITY TRANSPORTATION CENTER
U.S. DEPARTMENT OF TRANSPORTATION

Innovative Bio-Mediated Particulate Materials for Sustainable Maritime Transportation Infrastructure

11/01/2015 to 6/30/2017

Lin Li (PI)
Shihui Liu (GRA)
Kejun Wen (GRA)
Dept. of Civil & Environmental Engineering
Jackson State University
Jackson, Mississippi

8/15/2017

FINAL RESEARCH REPORT
Prepared for:
Maritime Transportation Research and Education Center

University of Arkansas
4190 Bell Engineering Center
Fayetteville, AR 72701
479-575-6021

ACKNOWLEDGEMENT

This material is based upon work supported by the U.S. Department of Transportation under Grant Award Number DTRT13-G-UTC50. The work was conducted through the Maritime Transportation Research and Education Center at the University of Arkansas.

1. Project Description

The mechanical properties of sandy soils in the coastal area and beach sands often do not satisfy construction expectation for maritime transportation infrastructure. The salty, loose sand makes it difficult for quick construction of port, building and roadway. Sometimes the weakness and unpredictability of loose sand properties can lead to unexpected collapse. Such large soil deformations can cause significant damage to constructions in the vicinity and potential loss of human life. With an ever growing demand for quick, safe, and green transportation construction, the need for sustainable construction materials in the coastal area is evident. Traditional construction materials, such as concrete, are not sustainable which have significant impact on the environment (Akiyama et al. 2012).

Biomineralization is a promising and environmentally innocuous technology to improve soil engineering properties. It naturally happens and is induced by nonpathogenic organisms that are native to the soil environment (DeJong et al. 2006). One common biomineralization process is microbial induced calcite precipitation (MICP), calcite precipitation act as an agent of cohesion which can bond sand grains together and improve the engineering properties of sand. This innovative field has the potential to meet society's ever-expanding needs through improving soil properties and perfecting soil durability. Especially, this technology is environmentally friendly. *Sporosarcina pasteurii* has been widely used for MICP due to its highly active urease enzyme, which catalyzes the reaction network towards precipitation of calcite (DeJong et al. 2006, Chou et al. 2011, Zhao et al. 2014a, Jiang et al. 2016, Pham et al. 2016, Li et al. 2017). This process produces dissolved ammonium and inorganic carbonate. The released ammonia subsequently increases pH, leading to accumulation of insoluble $CaCO_3$ in a calcium rich environment. The precipitated calcite can be used as bio-mediated cohesive material to particulate material.

MICP can provide unexplored opportunities for cost-effective, in situ improvement of the engineering properties of soil. As one of the natural process in mineral precipitation, MICP by urea hydrolysis can result in relatively insoluble compounds contributing to soil cementation. Previous research and testing has focused almost exclusively on the standard Ottawa silica sands due to its uniform pore size. As a result, little is known on the more problematic cases of sandy soils in the coastal area and beach sands for the bio-mediated soil improvement. The much finer structure and durability are two unknown factors for the MICP (Li et al. 2017).

Strength and durability are two among several key engineering properties of MICP-treated sands for using as maritime transportation infrastructure. Durability, which can be defined as the ability of a material to retain stability and integrity over years of exposure to the destructive forces of weathering, is one of the most important properties. MICP-treated sandy soil is a kind of porous brittle material. In moist environment, the repeated wetting and drying cycles should be a main reason for strength reduction of these materials. In cold environments, the freezing and thawing durability is especially important for a porous brittle material when it is

subjected to lower temperatures (Cai and Liu 1998, Li et al. 1999). The deterioration proceeds as freeze-thaw cycles are repeated, and the material gradually loses its stiffness and strength.

The primary objective of this research project is to develop bio-mediated particulate materials to enhance the resilience and protection of maritime transportation infrastructure elements. The advanced materials are based on MICP for the sandy soils in the coastal area and beach sands. A testing program was designed to test the MICP processes under biotic conditions and their durability.

2. Methodological Approach

2.1. Materials

To produce MICP-treated specimens, following materials were used in the experiments:

2.1.1. Sand

Ottawa silica sand (99.7%) shown in Figure 2-1(a) was used in the experiments. The sand is uniformly with a median particle size of 0.46 mm and no fines were included. It was classified as poorly graded sand based on the Unified Soil Classified System.

The coast sand shown in Figure 2-1(b) used in the experiments was obtained from Biloxi Beach, Mississippi (named as Biloxi beach sand in the report). Its median particle size was 0.32 mm. It was classified as well poorly graded sand in accordance with the Unified Soil Classification System.

Figure 2-2 shows the particle size distribution of Ottawa silica sand and Biloxi beach sand. The Biloxi beach sand is finer than the Ottawa sand.

2.1.2. Bacteria

As shown in Figure 2-3, *S. pasteurii* (ATCC 11859) was used in the experiments. The bacteria was cultivated in ammonium-yeast extract media (growth media; ATCC 1376), which is constituted by following per liter of deionized water: (1) 0.13 M tris buffer (pH = 9.0), (2) 10 g $(NH_4)_2SO_4$, and (3) 20 g yeast extract. The bacteria and growth media were centrifuged at 4,000 g for 20 min after incubating aerobically at 30^0C in a shaker at 200 revolutions per min overnight. Then supernatant was removed and replaced with fresh growth media before the bacteria was re-suspended every time. The bacteria were grown for 24–28 hrs to an optical density (OD) of 600 nm (OD_{600}) of 0.3–1.5 (10^7–10^8 cells/mL). The bacteria and growth media were stored in centrifuge vials at 4 ℃ until used (Mortensen et al. 2011).

(a)

(b)

Figure 2-1 Unconsolidated sand (a) Ottawa silica sand; (b) Biloxi beach sand

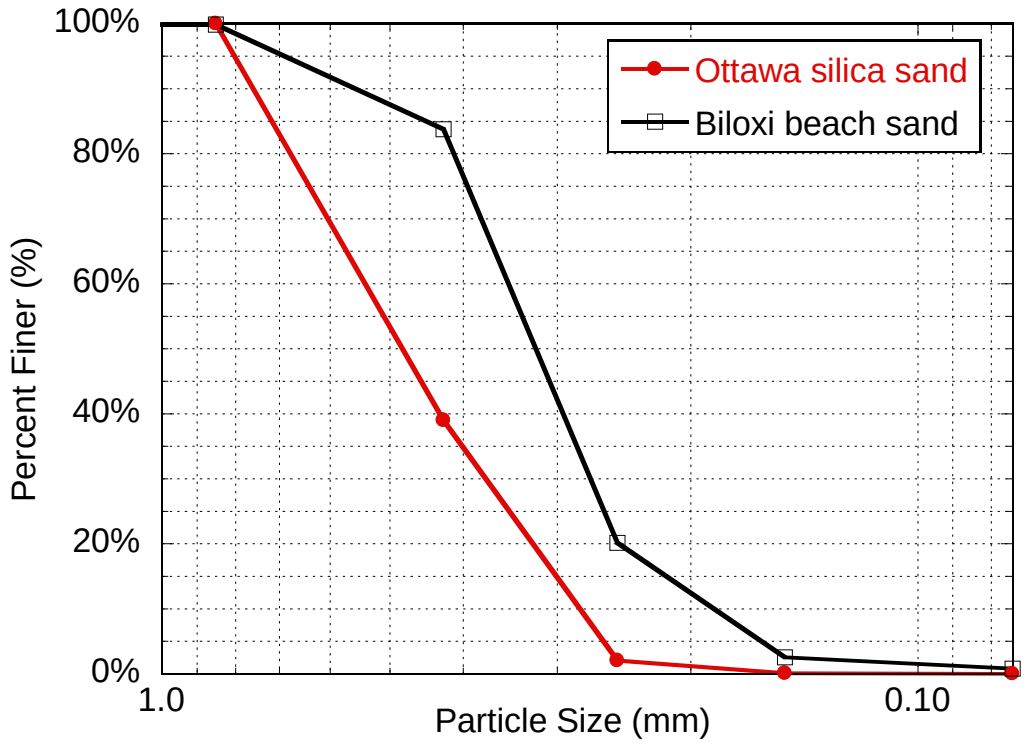

Figure 2-2 Particle size distribution of Ottawa silica sand and Biloxi beach sand

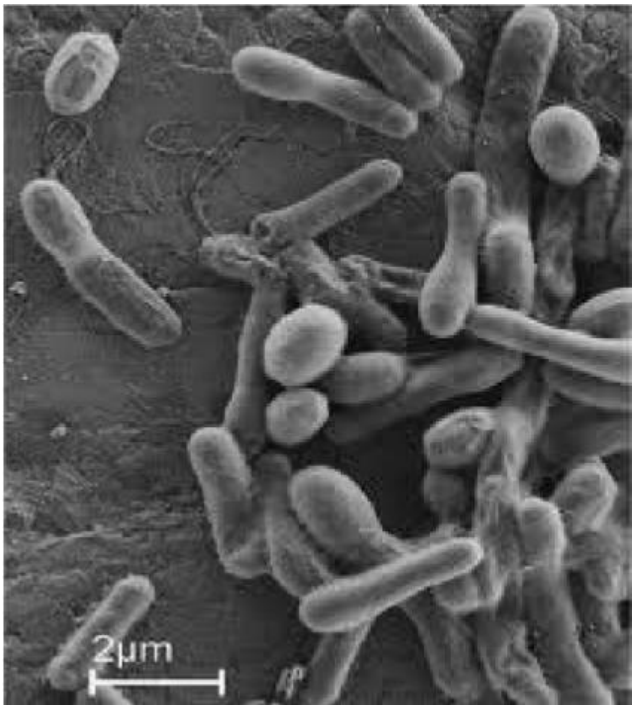

Figure 2-3 Bacteria *Sporosarcina pasteurii* used in this study (reprinted from Bang, 2015)

2.1.3. Full Contact Flexible Mold (FCFM)

The MICP-treated specimens were prepared by full contact flexible molds, which are made of geotextile. The geotextile is a polypropylene, staple fiber and needle punched nonwoven material. The fibers are needle punched to form a stable framework that retains dimensional stability relative to each other. Five types of geotextiles were used in this study which are labeled as G1, G2, G3, G4, and G5 (Figure 2-4). Their properties, such as grab tensile strength, apparent opening size, thickness, unit mass, are different (Table 2-1).. For example, the geotextile G2 has a grab tensile strength of 1689 N, grab elongation of 50%, trapezoidal tear of 667 N, apparent opening size of 0.15 mm, water flow rate of 34 mm/s, thickness of 1.51 mm, and unit mass of 200 g/m^2. These geotextiles have a large number of pores, promoting penetration of nutrients, urea, and calcium chloride into the sand pores and result in increased contact between the cementation solution and the bacteria, which is beneficial to the MICP process. Furthermore, the geotextile mold can provide a large attachable area, which attracts a portion of the calcium carbonate precipitated on its surface and reduces precipitation in the sand pore space and on the sample surface.

The size of the unconfined compression test mold is 38.1-mm diameter and 76.2-mm height. The molds consist of an annular part, a bottom, and a cover. The appearance of full contact flexible mold for unconfined compression tests samples is shown in Figure 2-5.

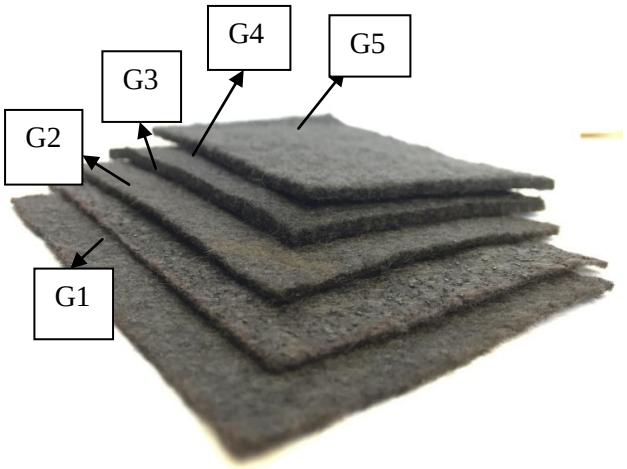

Figure 2-4 Photograph of five types of geotextile

2.1.4. Fiber

Fibermesh 150 shown in Figure 2-6 was used in this study to improve the ability for MICP-treated sand to resist wet-dry cycles. It is a 100% uniform homopolymer poly-propylene

multifilament fiber with a specific gravity (*Gs*) of 0.91. It is chemically inert with high acid salt resistance. The length and thickness of the fibers used in this study are 12 mm and 0.1 mm, respectively, with an aspect ratio of 120 between the length and thickness of the fiber. Consoli et al. (2009) used similar fibers of different lengths for the reinforcement of sand. It was concluded that fibers with an aspect ratio above 300 experienced strain hardening behavior, which caused significant mechanical problems such as fracture failures during shearing of the soil and a significant decrease in the ductility behavior of the fiber. The aspect ratio of the fiber used in this study was lower than the upper limit determined in the previous studies, indicating that it should provide efficient reinforcing performance (Consoli et al. 2009).

Table 2-1 Properties of geotextiles*

Parameter	Mechanical Properties			Physical Properties		Thickness (mm)	Unit Mass (g/m^2)
	Tensile Strength (N)	Trapezoidal Tear (N)	CBR Puncture (N)	Apparent Opening (mm)	Water Flow Rate (mm/s)		
Test Method	ASTM D-4632	ASTM D-4533	ASTM D-6241	ASTM D-4751	ASTM D-4491		
G1	455.02	200.02	1379.25	0.21	57.04	1.07	162.5
G2	1689.23	666.79	4556.31	0.15	33.95	1.51	200.0
G3	911.99	356.03	2335.83	0.18	36.67	1.91	262.5
G4	1690.01	643.96	4560.43	0.15	20.37	2.57	562.5
G5	1690.99	622.99	4560.43	0.15	20.37	2.91	525.5

* All the data are provided by manufacturers

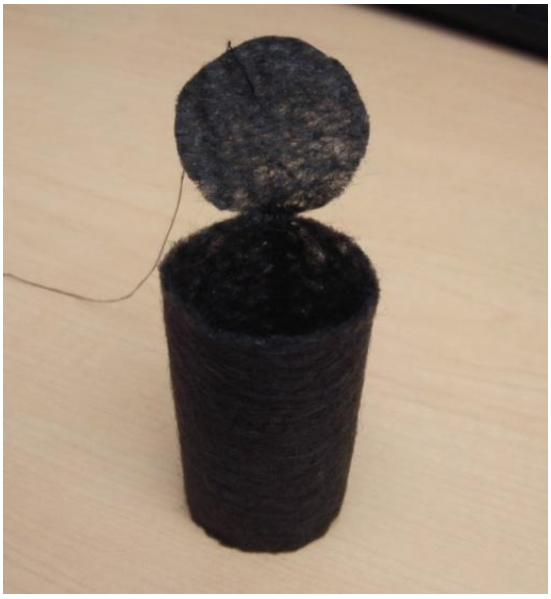

Figure 2-5 Photograph of full contact flexible mold for MICP

Figure 2-6 Photograph of synthetic fibers used in this study

2.2. MICP samples preparation

2.2.1. Cementation media

Cementation media was used to provide chemical compositions for ureolysis, including urea, $CaCl_2$ $2H_2O$, NH_4Cl, $NaHCO_3$, and nutrient broth (Mortensen et al. 2011). Four different cementation media concentrations were prepared. Table 2-2 summarizes the chemical compositions of the four different cementation media concentrations. The urea-Ca^{2+} molar ratio was 1: 1. The pH of the cementation media maintain in 6.0 at the beginning of the MICP process.

Table 2-2. Chemical compositions for cementation media.

Chemical	Chemical concentration (g/L)			
	0.25 M Ca	0.5 M Ca	1 M Ca	1.5 M Ca
NH_4Cl	10.0	10.0	10.0	10.0
Nutrient broth	3.0	3.0	3.0	3.0
$NaHCO_3$	2.12	2.12	2.12	2.12
Urea	15.0	30.0	60.0	90.0
$CaCl_2 \cdot 2H_2O$	36.8	73.5	147.0	220.5
pH	6.0	6.0	6.0	6.0

2.2.2. Batch Reactor

All samples were prepared in completely stirred tank reactor. The reactor shown in Figure 2-7 included a plastic box to contain soil samples and cementation media, a magnetic mixer to keep the solution uniform, and an air pump to provide oxygen for bacteria. A major feature of this method is to allow soil samples fully immerse into the cementation media and to allow the cementation media to freely penetrate into the soil samples instead of using pump to inject cementation media.

As the cementation media permeates into the soil specimens, MICP can occur in sample pores and the produced $CaCO_3$ can bond the sand particles together to improve the engineering properties. Many studies have used pump to inject cementation media into sample pores to promote the MICP process in samples. Using this method, the $CaCO_3$ content often varied in specimens along the direction of the cementation media flow and even sometimes clogged the soil pore spaces near the injection point (Stocks-Fischer, Galinat et al. 1999, Whiffin et al. 2007). In this study, the samples were prepared by the FCFM and immerged into cementation media in a batch reactor. The chemical substances freely diffuse into the sample space under the action of magnetic stirrer. Zhao et al. (2014a) found that the produced $CaCO_3$ was fairly distributed in the samples and the samples could be easily taken out from mold for different tests.

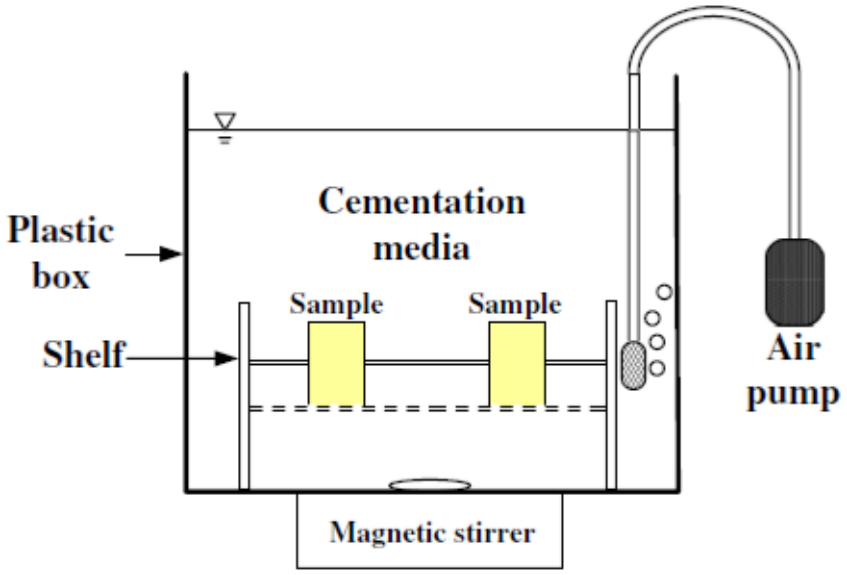

Figure 2-7 Sketch of Batch Reactor for MICP

In the batch reactor, there is not hydraulic gradient to drive the flow through the soil specimen. The hydraulic conductivity of the MICP-treated sand is in the range of 0.001 cm/s, which is permeable to cementation media. When the chemical of cementation media reacts under

the catalysis of bacteria, the concentration of these chemicals is lower in the soil specimens, which causes the chemical substances diffuse from high concentration area to low concentration area to continue the MICP deeper in the soil specimens.

2.2.3. Sample preparation

The samples of FCFM for unconfined compression tests, 140±5 g sand was uniformly mixed with 45-mL bacteria solution and then air pluviated into the mold to reach a median dense condition (D_r in the range of approximately 42–55%, and dry density of sand ranged from 1.58–1.64 g/cm^3). Placed the samples on the shelf (shown in Figure 2-8(a)) and then immerged the entire shelf into the batch reactor filled with cementation media. Following methods of Zhao et al. (2014a), the MICP process will maintain for 7 days without adding any additional cementation media, bacteria, or growth media. The shelf and samples will be removed from the reactor at the end of the reaction time (Figure 2-8(b)). Then, the MICP-treated specimens were removed from the molds by cutting the molds and stored samples in 50^{0}C constant temperature oven to dry for 48 hrs before testing. At least four samples were prepared for each case to produce a representative condition in the experiments.

2.3 Methods

2.3.1 MICP-treated specimens aging

The durability of MICP-treated specimens was evaluated by testing the aged samples. The MICP-treated specimens were aged in two different conditions, separately, (1) one to five wet-dry cycles to simulate the change of moist in natural environment; and (2) five to fifteen freeze-thaw cycles to simulate the effect of temperature changes on the performance of the MICP-treated specimens.

(1) Wet-dry cycles

There is no standard testing method to perform wet-dry cycles for MICP-treated specimens. Consequently, ASTM D559-15 was adopted for tests of wet-dry cycling of MICP-treated specimens. These samples were subjected to one to five wet-dry cycles. In each cycle, the samples were submerged in water shown in Figure 2-9 for 24 hrs and then were dried in 50^{0}C for 48 hrs to permit the dissipation of the excess moisture. The samples were then tested for their unconfined compressive strength (UCS) and compare with unweathered samples to determine strength impact on the MICP-treated specimens.

(a)

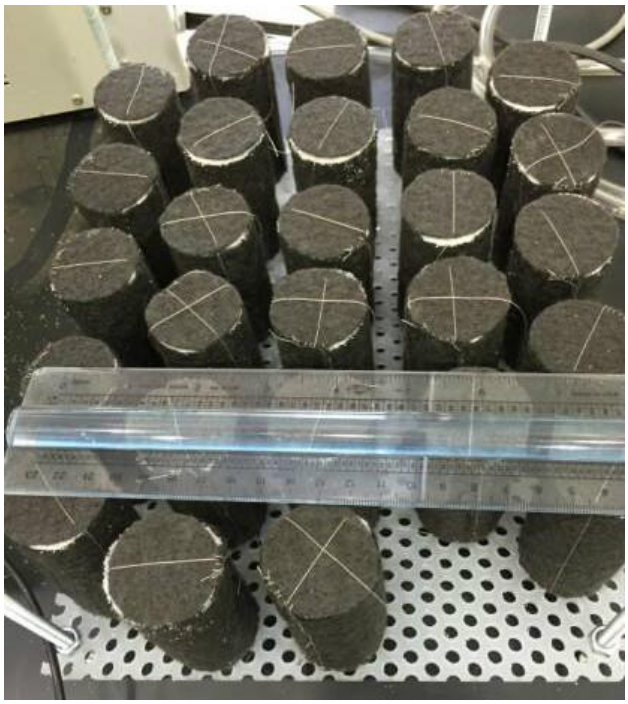

(b)

Figure 2-8 Photograph of specimens in the full contact flexible molds: (a) before the reactions; (b) after the MICP reactions. The full contact flexible mold was fabricated by geotextile. PVC shelf was used to support full contact flexible molds.

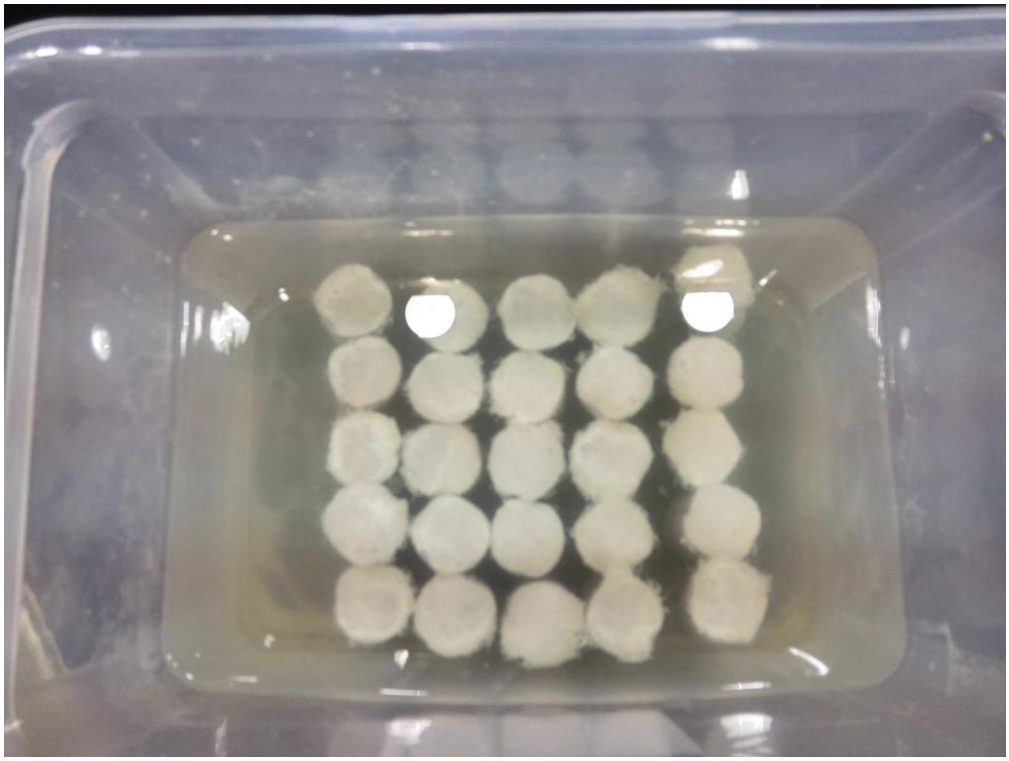

Figure 2-9 Photograph of MICP-treated specimens submerged in water during the wetting process

(2) Freeze-thaw cycles

There is no standard testing method to perform freeze-thaw cycles for MICP-treated specimens. Consequently, the ASTM D560-16 was adopted for freeze-thaw cycling of MICP-treated specimens. The samples were frozen in -18^0C for 24 hrs and then were thaw in a laboratory environment (i.e., 20^0C $\pm$ 2^0C). The samples were then tested for their UCS and compare with unweathered samples to determine strength impact on the MICP-treated specimens.

2.3.2 Unconfined compression strength tests

The unconfined compression tests were conducted under strain controlled conditions at a uniform loading rate of 1.5%/min in accordance with ASTM D2166/D2166M-13 (ASTM 2013). Figure 2-10 illustrates the laboratory setup of UCS test.

2.3.3 $CaCO_3$ content

To determine precipitated $CaCO_3$ in the MICP-treated specimens, crushed samples were oven-dried for 48 hrs to permit the dissipation of the excess moisture. The dry samples were washed in HCl solution (0.1 M) to dissolve precipitated carbonates, rinsed, drained, and oven-

dried for 48 hrs. The difference between these two masses is considered to be the mass of the carbonates that were precipitated in the specimens and molds.

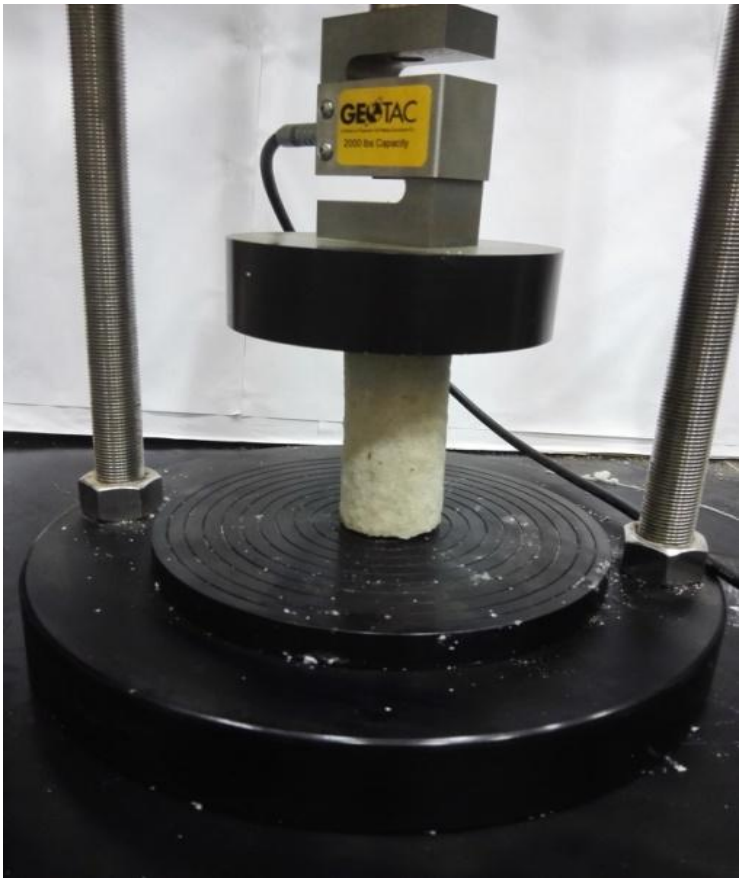

Figure 2-10. Laboratory setup of unconfined compression tests

2.3.4 Scanning Electron Microscopy

The formation of MICP was examined by scanning electron microscopy (SEM). The MICP-treated specimens were sputter-coated for SEM analysis. The chemical composition of samples was also analyzed using energy dispersive X -ray analyzer (EDX).

3. Results/Findings

3.1 Effect of geotextile type on the FCFM

Five different geotextile materials were used to prepare the full contact flexible mold. Figure 3-1 shows a box plot of unconfined compression strength as a function of geotextile type. Each box shows the median value and ±25% of the UCS population as the top and bottom of the box. The lines extending from the top and bottom of each box mark the minimum and maximum

UCS. The outlier is shown as an individual point. The median UCS of samples packed by G1 and G2 are 1.15 MPa and 1.05 MPa, respectively. The G1 is the thinnest geotextile among the five geotextile material. With the tensile strength of 455.02 N, and trapezoidal tear of 200.02 N, the geotextile mold made with G1 was difficult to maintain the cylinder shape when the sand is filled in. The geotextile mold made from G2, G3, G4, and G5 are well-maintained cylinder shape when the sand is filled in. Those cylinder shaped MICP-treated specimen is prerequisite for the unconfined compression strength tests. The UCS of samples made by G3, G4, and G5 decreased from that of G2. The thicker geotextile mold made by G3, G4, and G5 reduces the infiltration effect on the MICP, compared to that of G2. Therefore, geotextile of G2 was selected to make FCFM in the following experiments.

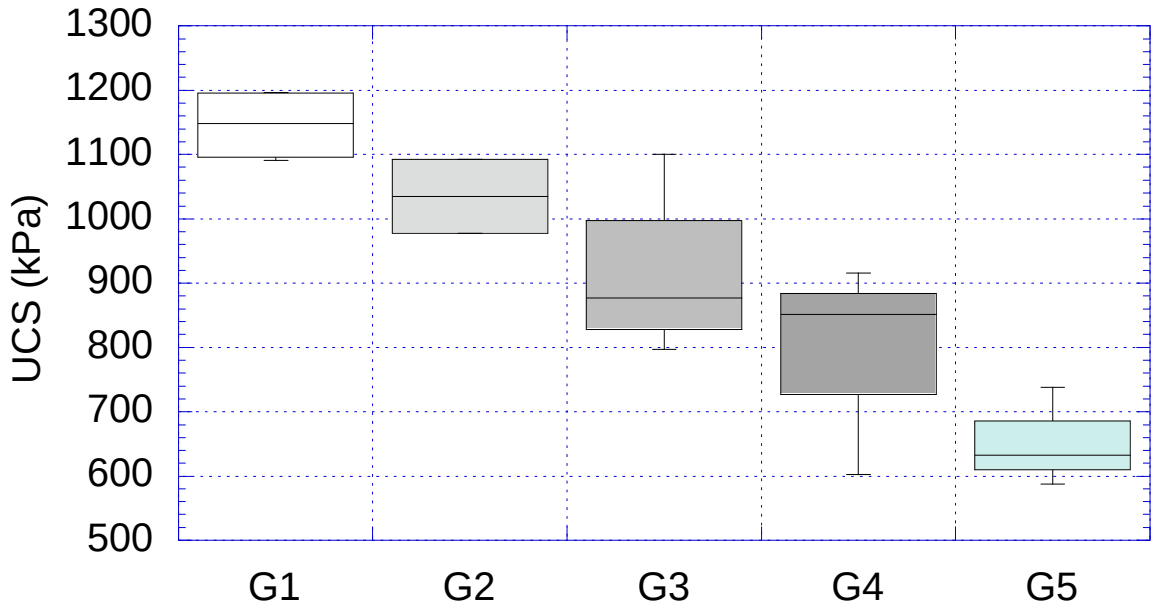

Figure 3-1 Box plot of UCS of MICP-treated specimens as function of geotextile types in the mold. The OD_{600} was set at 0.6, and the cementation media concentration was set at 0.5 M.

The SEM image in Fig 3-2(a) and (b) shows that the formed $CaCO_3$ crystals were mainly irregular bulk in the MICP-treated specimen in geotextile mold G2, that observations are similar to Qabany et al. (2012). However, the crystal size (10~100 μm) was obviously larger than the size indicated in their results, probably due to the different sample preparation method. This study used FCFM to prepare the soil specimen by immerging the sample into cementation media. These MICP-treated sand specimens could be taken out from mold for different mechanical tests. With the full contact flexible mold preparation, the $CaCO_3$ in the MICP-sand specimen was more evenly distributed in samples.

3.2 Effect of bacteria concentration

Five different bacteria concentrations were used MICP-treated soil catalyzed by *S. pasteurii*. Table 3-1 shows the urease activity and specific urease activity of the bacteria, $CaCO_3$ content, and UCS under different OD_{600}. The OD_{600} represents the concentration of bacteria, urease activity reflects the catalytic ability of bacteria hydrolyzing urea, and the specific urease activity illustrates the catalytic ability of unit bacteria hydrolyzing urea. As the OD_{600} value increases, the urease activity gradually rises, but the specific urease activity only increased rapidly when the OD_{600} increased from 0.3 to 0.6. After the OD_{600} reached 0.6, the increase in specific urease activity becomes slow.

Although *S. pasteurii* can constitutively produce high levels of urease theoretically (Mörsdorf and Kaltwasser 1989), Whiffin (2004) found that no correlation existed between urease activity and biomass. Whiffin (2004) indicated that the urease was not produced constitutively and was affected by many factors, resulting in the variation of specific urease activity. Figure 3-3 shows a box plot of UCS as a function of bacteria concentration (OD_{600}). With more bacteria, the $CaCO_3$ content and median UCS of MICP-treated specimens increase. The increase in $CaCO_3$ content results in an increased strength in the MICP-treated specimens. The range of UCS under different OD_{600} is similar, except when the OD_{600} is 1.5. The increase in UCS is consistent with the increase in urease activity and $CaCO_3$ content (Table 3-1). The OD_{600} of the bacteria growth media in this study was approximately 0.6 for bacteria concentrations of approximately 4.28×10^7 cells/mL.

(a) (b)

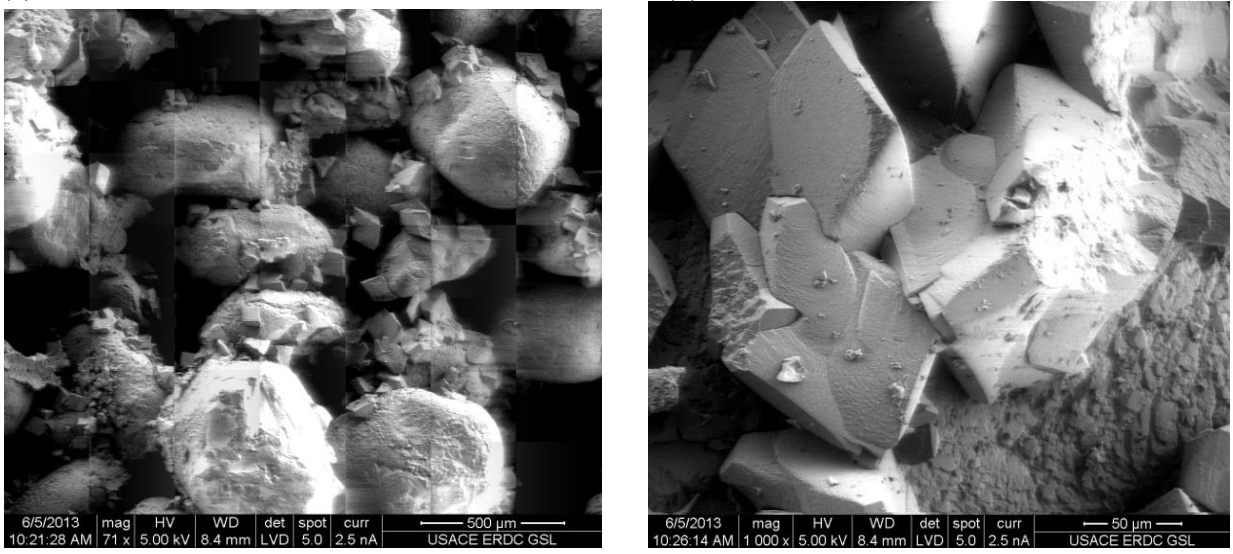

Figure 3-2 SEMs of MICP-treated specimens catalyzed by *S. pasteurii* (a) Sand and $CaCO_3$ crystals; (b) precipitated $CaCO_3$ crystals. The specimens were prepared at the G2 geotextile mold and in the bacteria solution of 0.6 OD_{600}, and the cementation media concentration of 0.5 M.

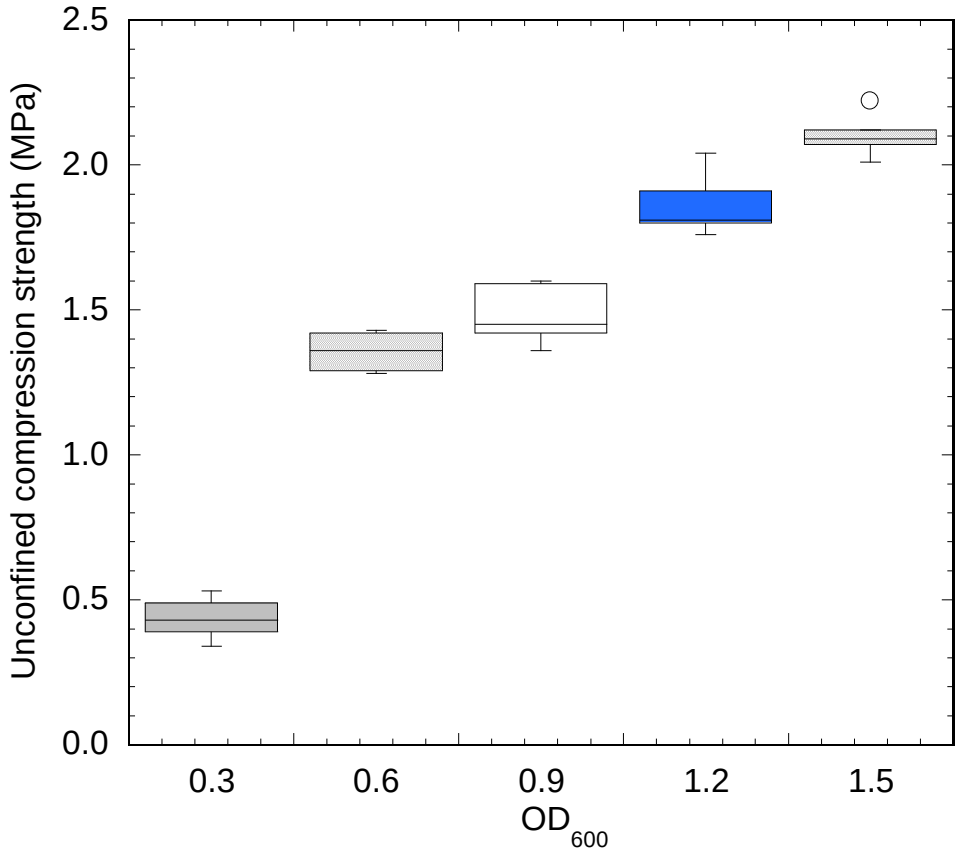

Figure 3-5 Box plot of unconfined compression strength of MICP-treated specimens catalyzed by *S. pasteurii* as a function of OD_{600}

Table 3-1. Urease activity, specific urease activity, $CaCO_3$ content and UCS under different OD_{600} of MICP-treated specimens catalyzed by *S. pasteurii*

OD_{600}	0.3	0.6	0.9	1.2	1.5
Urease activity	1.14	3.31	5.27	6.90	8.85
Specific urease activity	3.81	5.52	5.85	5.75	5.90
$CaCO_3$ content (%)	4.88~5.19	7.21~7.88	8.57~9.45	10.14~11.36	13.09~14.44
UCS (MPa)	0.34~0.53	1.28~1.43	1.36~1.60	1.76~2.04	2.01~2.22

Note: Urease activity (mM hydrolysed urea/min), and specific urease activity (mM hydrolysed urea/min/OD). The specific urease activity = urease activity/OD_{600}

3.3 Effect of cementation media concentration

To investigate the effect of cementation media concentration on MICP-treated sand, the sand samples was prepared under four different cementation media concentrations with the

OD_{600} of 0.6. The chemical compositions of the four different cementation media concentrations are summarized in Table 2-2. Table 3-2 summaries the UCS and $CaCO_3$ content of the MICP-treated specimens under the four different cementation media concentrations. The results show that UCS and $CaCO_3$ content of the MICP-treated specimens increases with urea and calcium ions in cementation media during the MICP process. When cementation media concentration increased from 0.25 to 0.5 M Ca, the median UCS increased from 0.13 MPa to 1.36 MPa, which is almost one order of magnitude. However, when cementation media concentration increased from 0.5 MPa to 1.5 M Ca, the median UCS became double from 1.36 MPa to 2.13 MPa. This observation shows that urea and calcium ions in cementation solution have not been fully utilized when its concentration is higher than 1 M Ca. This is probably because the MICP process was limited by enzyme quantities and reached the maximum ability of urea hydrolysis, or the high concentration of calcium chlorine in cementation solution reduced the urease activity of bacterial enzyme (Whiffin 2004, Van Paassen 2009). Although a high concentration of cementation media can improve MICP treatment effect and mechanical properties to some extent, only a portion of calcium ions was precipitated by MICP. The results indicate that the sole increase in concentration of cementation media is a limited method to enhance MICP.

Table 3-2. $CaCO_3$ content and UCS under different cementation media concentrations of MICP-treated specimens catalyzed by *S. pasteurii*

Cementation media concentrations	*S. pasteurii*	
	$CaCO_3$ content (%)	UCS (MPa)
0.25 M Ca	1.90~2.02	0.08~0.18
0.5 M Ca	7.21~7.88	1.28~1.43
1.0 M Ca	9.56~11.12	1.60~2.10
1.5 M Ca	12.14~13.39	2.04~2.13

where OD_{600} = 0.6

3.4 Durability results of MICP-treated specimens during the various wet-dry cycles

3.4.1 Unconfined compressive strength results

The stress–strain curves obtained from UCS tests on MICP-treated sand specimens through different wet-dry cycles is shown in Figure 3-6. Although the MICP-treated samples can reach a fairly uniform state in the full contact flexible mold, there was still slightly different $CaCO_3$ content distributed within each sample, which may cause strength fluctuate during the tests. At least four samples were prepared for each case to produce a representative condition. With the wet-dry cycles, the unconfined compression strength for MICP-treated Ottawa silica sand decreases (Figure 3-6(a)). The peak strength of unweathered samples is about 1.3 MPa. The peak strength dropped to 0.25 MPa after one wet-dry cycle. The drop is very significant with

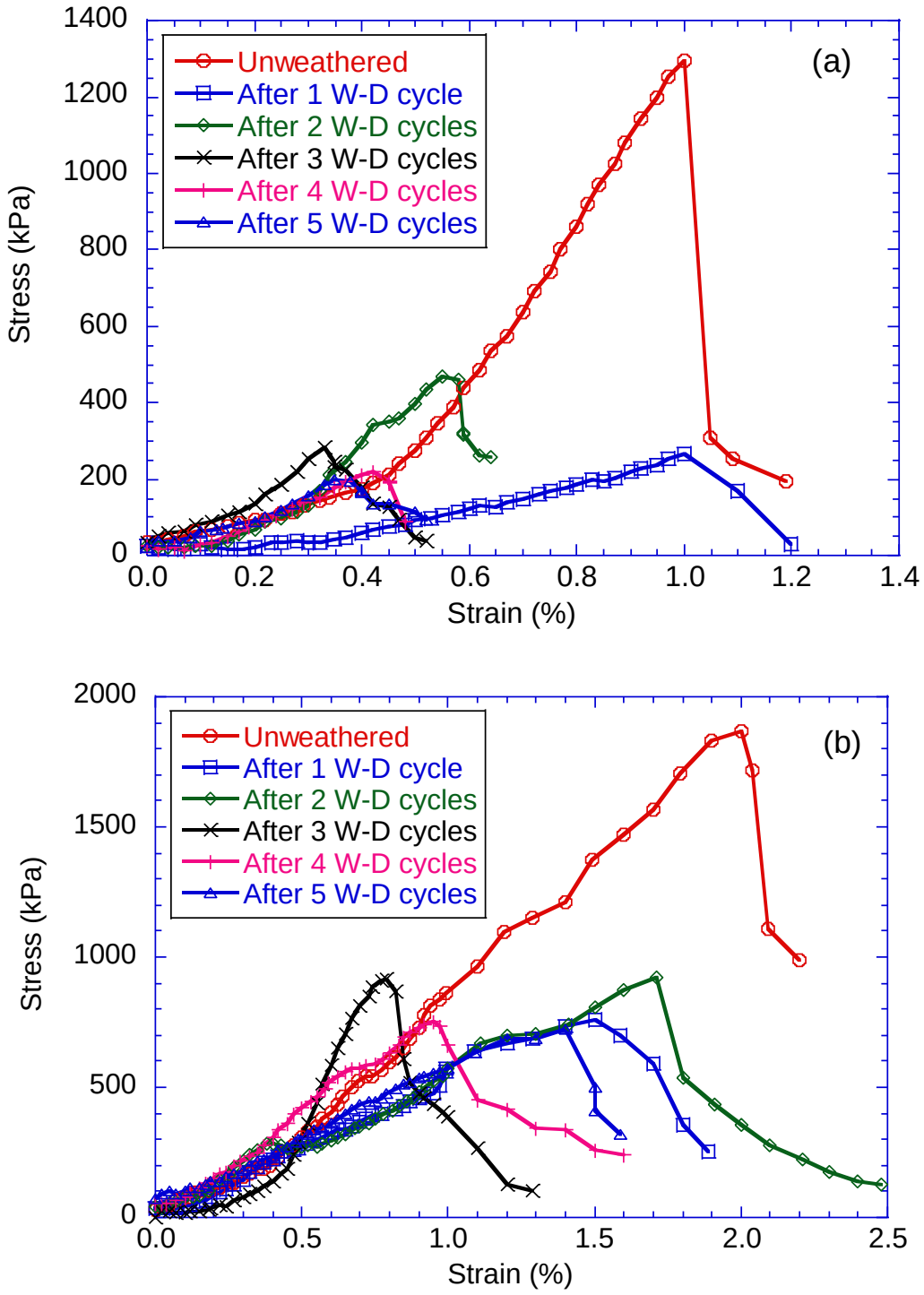

Figure 3-6 Stress-strain relationship of MICP-treated sand samples as a function of wet-dry cycles (a) Ottawa silica sand; (b) Biloxi beach sand. The specimens were prepared with the G2 geotextile mold and in the bacteria solution of 0.6 OD_{600}, and the cementation media concentration of 0.5 M.

nearly 420% decreasing of ultimate strength. The strain at the peak strength did not change too much (around 1.0%). The decreasing of peak strength in the one cycle of wet-dry period is caused by the soften calcite after soaking with water in the wetting procedure, then the strength of soften calcite reduces after the drying period. However, when the second wet-dry cycles was applied to the MICP-treated sample, the peak strength bounced back to 0.45 MPa, but the strain at the peak strength decreased from 1.0% to 0.55%. The bounced back of peak strength in the second wet-dry cycle is caused by the hardening calcite formed in the MICP-treated sample. The decreasing strain after the second wet-dry cycle demonstrates the strain hardens phenomena. The MICP-treated samples became more brittle after the second wet-dry cycles. With more cycles of wet-dry (3, 4 or 5 cycles of wet-dry), the peak strength of MICP-treated samples decreases and tends to reach stable after the four cycles of wet-dry with relative stable peak strength (0.2 MPa and failure strain at 0.4%).

Figure 3-6(b) shows the stress-strain relationship of UCS for MICP-treated Biloxi beach sand samples. The peak strength of unweathered samples is about 1.9 MPa, then it dropped to 0.75 MPa after 1 cycle of wet-dry. Then the peak strength bounced back to 0.89 MPa after the second wet-dry cycle. After the third cycle of wet-dry, the peak strength of MICP-treated Biloxi beach sand samples continuously decrease to 0.8 MPa, to 0.76 MPa (after 4 cycles of wet-dry) and to 0.72 MPa (after 4 cycles of wet-dry). The behavior of MICP-treated Biloxi beach sand samples is similar to MICP-treated Ottawa sand samples in the wet-dry cycle.

Table 3-3 UCS of MICP-treated sand before and after wet-dry cycles

Sand Type	Average UCS of unweathered samples (MPa)	Times of wet-dry cycles	Average UCS of weathered samples (MPa)	UCS loss rate (%)*
Ottawa silica sand	1.24	1	0.23	81.45
		2	0.43	65.32
		3	0.27	78.23
		4	0.21	83.06
		5	0.18	85.49
Biloxi beach sand	1.88	1	0.73	61.17
		2	0.87	53.72
		3	0.77	59.04
		4	0.70	62.77
		5	0.56	70.21

Note: *UCS loss rate (%) = 100 – (Average UCS of weathered samples (MPa)/Average UCS of unweathered samples (MPa))x100

Table 3-3 shows the UCS loss rate of MICP-treated specimens after wet-dry cycles. For Ottawa silica sand, the peak strength dropped sharply after 1 cycle. After the UCS bounced back

in the second wet-dry cycle, the UCS decreased along with more wet-dry cycles. The total UCS lost after five cycles of wet-dry was 85.5% of initial strength compared with the unweathered samples. For Biloxi beach sand, the peak strength after MICP treatment lost 61% after 1 cycle. After the UCS bounced back to 53.7% of initial strength in the second wet-dry cycle, the UCS decreased along with more wet-dry cycles. The total UCS lost after five cycles of wet-dry was 70.2% of initial strength compared with the unweathered samples. In the durability of wet-dry environment, MICP-treated beach sand samples had the same trend as Ottawa silica sand. However, MICP-treated Biloxi beach sand shows a better ability to resist the wet-dry cycles, where the samples still had about 29.8% of initial strength remained after five cycles of wet-dry. For comparison, MICP-treated Ottawa silica sand samples only had 14.5% of initial strength remained after five cycles of wet-dry.

Box plot of UCS of MICP-treated samples as a function of weathered number in wet-dry cycles is shown in Figure 3-7. Each box shows the median value and ± 25% of the UCS population as the top and bottom of the box. The lines extending from the top and bottom of each box mark the minimum and maximum UCS. The outlier is shown as an individual point. For MICP-treated Ottawa silica sand samples (Figure 3-7(a)) and MICP-treated Biloxi beach sand samples (Figure 3-6(b)), the UCS of MICP-treated specimens decreased obviously after one cycle of wet-dry. With similar decreasing pattern of the two type of soil, the MICP-treated samples become brittle and weak in the wet-dry environment.

3.4.2 Attenuation coefficient

To show the effect of the wet-dry cycles on MICP-treated Ottawa silica sand and MICP-treated Biloxi beach sand, wet-dry attenuation coefficient is introduced. The wet-dry attenuation coefficient (η_w) is defined as the proportion of the unconfined compressive strength (q_u) before and after the wetting and drying treatment, which reflects the extent to which wetting and drying affect MICP-treated sand. The wet-dry attenuation coefficient formula is defined as follows:

(3.1)

where, q_{ui} is the initial unconfined compressive strength of samples before applying a wet-dry cycle, and q_{un} is the unconfined compressive strength of samples after applying *n* wet-dry cycles.

The wet-dry attenuation coefficient of MICP-treated Ottawa silica sand and MICP-treated Biloxi beach sand samples as a function of wet-dry cycles is shown in Figure 3-8. As shown in this figure, the wet-dry attenuation coefficients of both MICP-treated sand samples decline significantly after the first wet-dry cycle. The wet-dry attenuation coefficients of these two types of samples decreased gradually after 2 wet-dry cycles, and declined to 0.15 for MICP-treated Ottawa silica sand samples, and to 0.3 for MICP-treated Biloxi beach sand samples after 5 wet-dry cycles. This trend also indicates that MICP-treated sand were weak in wet-dry durability.

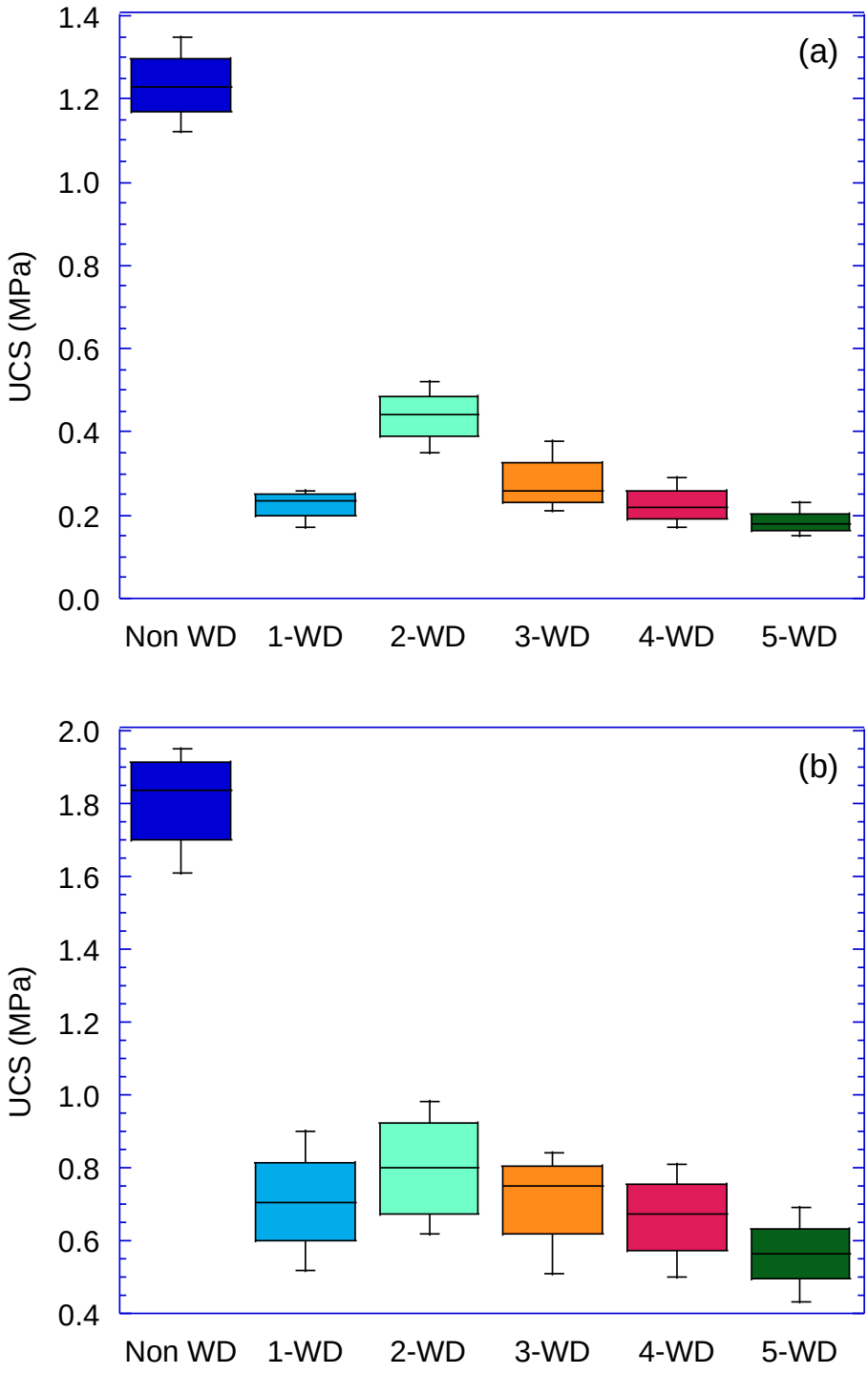

Figure 3-7 Box plot of UCS for MICP-treated sand samples as a function of wet-dry cycles (a) Ottawa silica sand; (b) Biloxi beach sand. The specimens were prepared with the G2 geotextile mold and in the bacteria solution of 0.6 OD_{600}, and the cementation media concentration of 0.5 M.

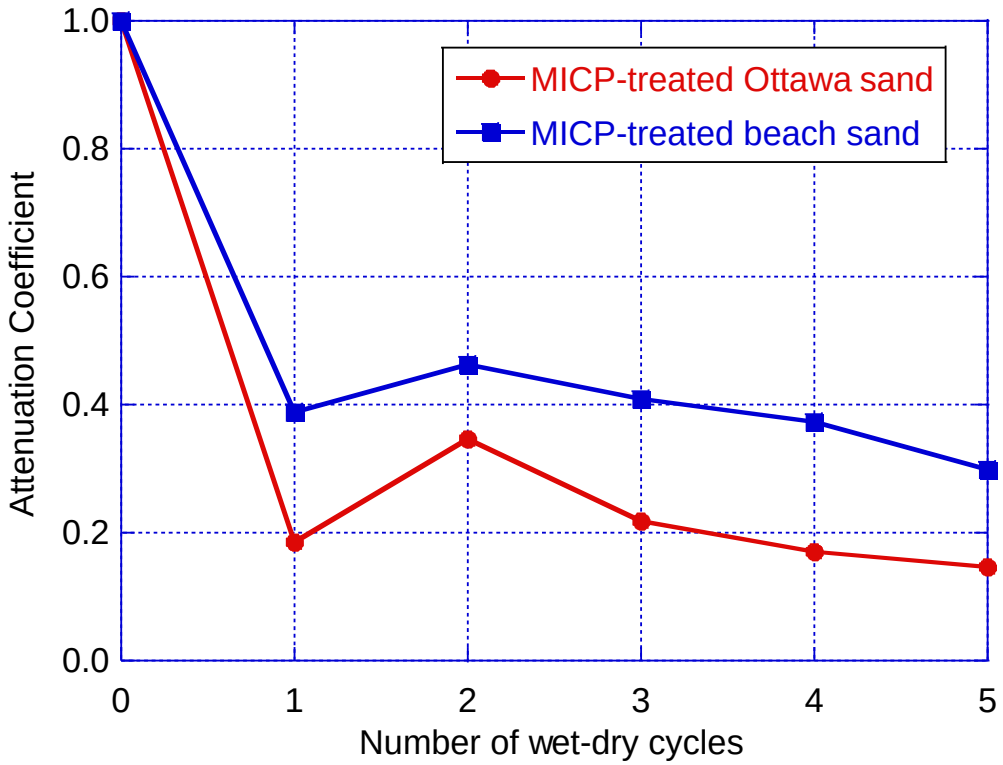

Figure 3-8 Attenuation coefficient of MICP-treated sand as a function of wet-dry cycles.

3.4.3 Improvement of MICP-treated sand to resist wet-dry cycles

Based on the results described above, MICP-treated sand was weak in wet-dry durability. To improve its ability of resisting wet-dry cycles, two methods were applied in this project: (1) discrete fiber reinforcement; and (2) multiple MICP treatment.

(1) Fiber reinforcement

The 140±5 g Ottawa silica sand and fibers (0.3% by weight of dry sand) were uniformly mixed with 45 mL bacteria solution and then air pluviated into the FCFM to reach a median dense condition (D_r in the range of 44–55%). In the preparation of all samples, the required bacteria solution was first added into the dry sand to prevent floating of the fibers in the soil matrix, and then the proposed content of fibers was mixed in small increments by hand to obtain a uniform mixture. It is important to ensure that all fibers are mixed thoroughly (Shao et al. 2014). Then put the samples on the shelf and immersed it into cementation media in the completely stirred tank reactor. After 7 days of MICP treatment, the shelf was removed from the solution, each geotextile mold was cut, and the MICP-treated specimens were removed. The unconfined compression tests were conducted after the samples were dried in 50^0C constant temperature oven for 48 hrs.

The stress–strain curves obtained from UCS tests on MICP-treated sand specimens with 0.3% fiber contents is shown in Figure 3-9. The peak strength of unweathered samples is about 1.1 MPa. After one cycle of wet-dry, the peak strength of reinforced MICP-treated sand dropped to 0.91 MPa. Compared to Figure 3-6 without fiber reinforcement, the loss of peak strength after one cycle of wet-dry is significant lower than that of without fiber reinforcement. As shown in Table 3-4, the fiber reinforced MICP-treated sand only lost 18% of initial peak strength, while the unreinforced MICP-treated sand lost 81% of initial peak strength. The failure strain of reinforced MICP-treated sand increased from 1.5% to 2.5% after one cycle of wet-dry. The results indicate the ductility of MICP-treated sand can be significantly improved by adding suitable amount of fibers (0.3% in this case). This finding is consistent with the results of past studies. Li et al. (2015) found that the inclusion of fibers is more effective at higher strain rates.

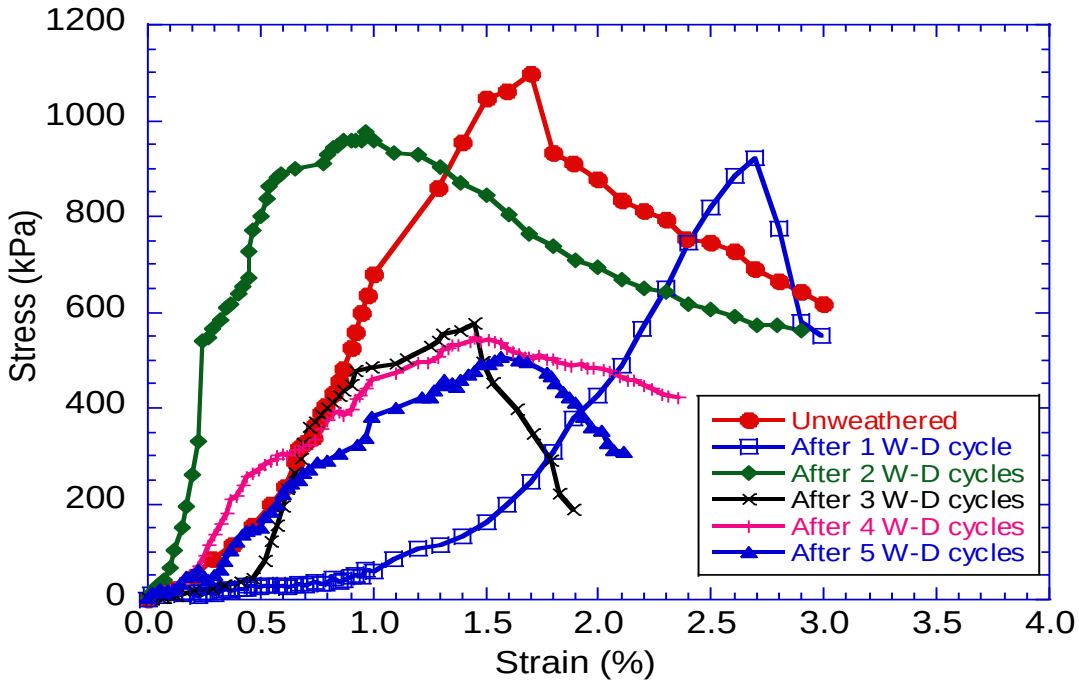

Figure 3-9 Stress-strain relationship of reinforced MICP-treated Ottawa silica sand with 0.3% fiber through various wet-dry cycles. The specimens were prepared with the G2 geotextile mold and in the bacteria solution of 0.6 OD_{600}, and the cementation media concentration of 0.5 M.

When the second wet-dry cycles, the peak strength reinforced MICP-treated sand bounced back to 0.97 MPa with 1.0% failure strain. As the more wet-dry cycles, the peak strength of reinforced MICP-treated sand decreases and the failure strain reduce along the wet-dry cycles. The peak strength dropped to 0.58 MPa, 0.56 MPa and 0.49 MPa, respectively, after 3 cycles, 4 cycles and 5 cycles of wet-dry. Box plot of UCS for fiber reinforced MICP-treated

Ottawa silica sand during wet-dry cycles is shown in Figure 3-10. It shows that fiber can slow down the decrease of peak strength in first two wet-dry cycles. The unconfined compressive strength attenuation coefficient results shown in Figure 3-11 also show a similar trend. However, the UCS of fiber reinforced MICP-treated sand sharply decreased after two wet-dry cycles. The results indicated that fiber can resist the weather durability for MICP-treated sandy soil in the beginning of wet-dry cycles. Once after two wet-dry cycles, the fiber reinforcement does not show any benefit to the strength of MICP-treated soil.

Table 3-4 UCS of reinforced MICP-treated sand with 0.3% fiber in various wet-dry cycles

Sand Type	Average UCS of unweathered samples (MPa)	Times of wet-dry cycles	Average UCS of weathered samples (MPa)	UCS loss rate (%)
Ottawa silica sand + 0.3% fiber	1.1	1	0.90	0.18
		2	0.98	0.11
		3	0.60	0.45
		4	0.58	0.47
		5	0.50	0.55

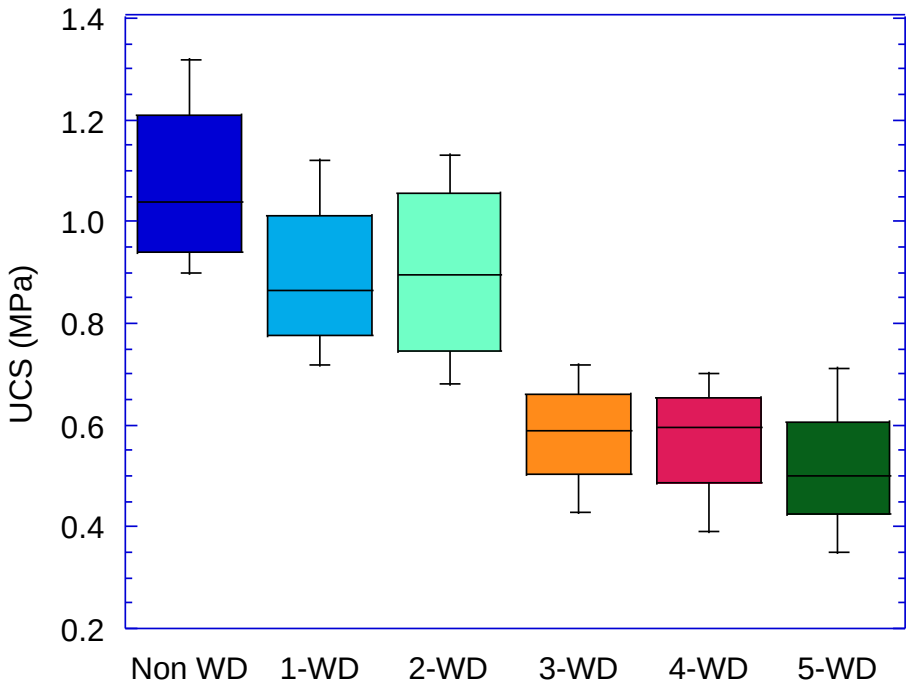

Figure 3-10 Box plot of UCS for reinforced MICP-treated Ottawa silica sand with 0.3% fiber after wet-dry cycles

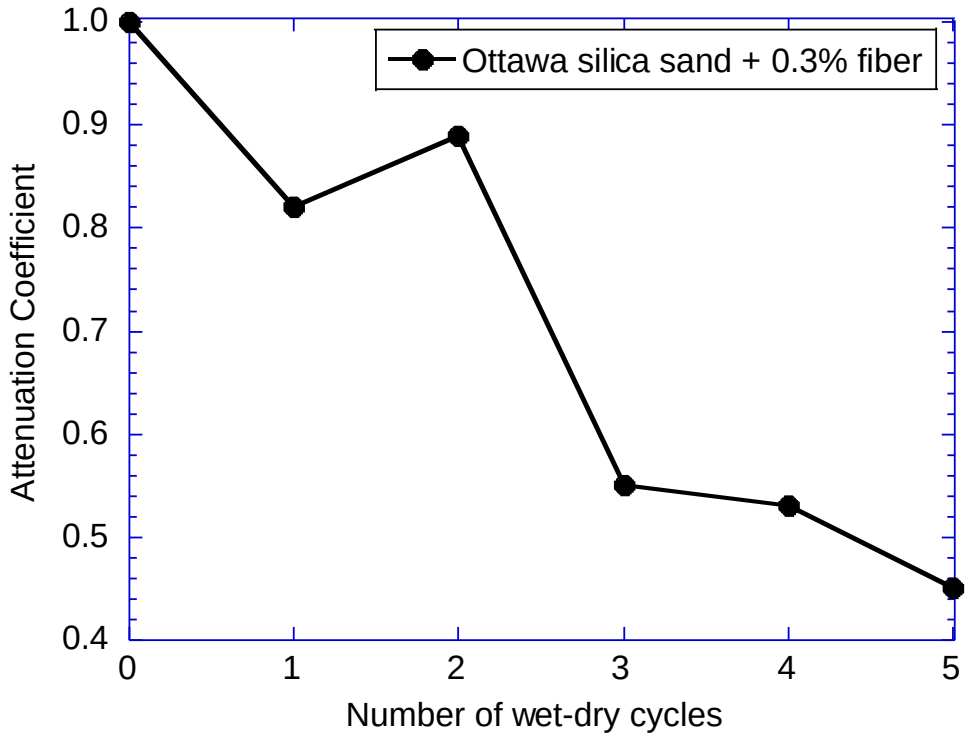

Figure 3-11 Attenuation coefficient of reinforced MICP-treated Ottawa silica sand with 0.3% fiber as a function of wet-dry cycles.

(2) Multiple MICP treatments

Multiple MICP treatments are referred to more than one time of treatment to induce MICP. After the first MICP treatment, the MICP-treated specimen was treated again with new bacteria, new growth medium, and new cementation medium for 7 day. Then the second-treated specimen was repeatly treated with new bacteria, growth medium and cementation medium for another 7 day. The maximum treatment times in this study was four times. The total treatment time is 28 days. The multiple MICP-treated samples were dried in 50^0C constant temperature oven for 48 hrs before the UCS tests.

The UCS results of multiple MICP-treated samples in one wet-dry cycle are shown in Figure 3-12. The UCS of single MICP-treated specimens dropped from 1.21 MPa to 0.2 MPa after 1 wet-dry cycle. But for the double MICP-treated specimens, the UCS almost maintained the same as 2.82 MPa. Along with the increase of MICP treatment times, the UCS of samples grew sustainably, it increase to 3.58 MPa and 4.24 MPa after triple and quadruple MICP treatment. Moreover, the UCS of weathered MICP-treated samples after the multiple treatments did not change much. Table 3-5 shows that the UCS loss rate for multiple MICP treatment samples is in a low level. Especially for quadruple MICP-treated samples, the loss rate was zero.

It indicates that multiple treatments could significantly improve the wet-dry durability of MICP-treated sandy soil.

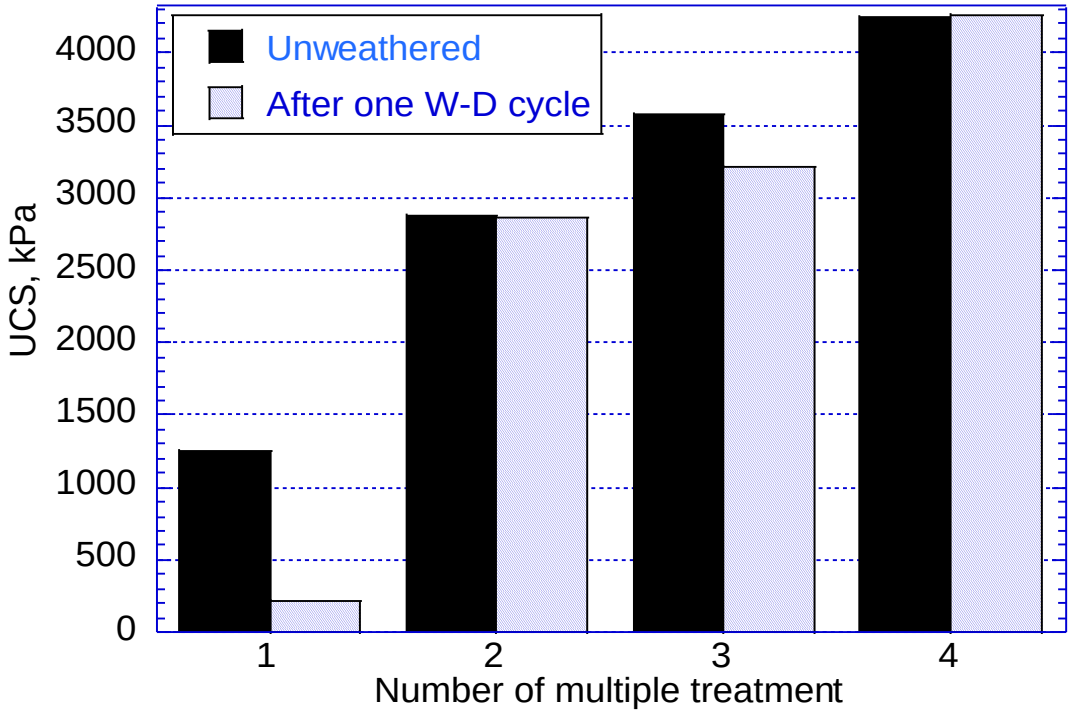

Figure 3-12 UCS of multiple MICP-treated Ottawa silica sand samples before and after one wet-dry cycle

Table 3-5 UCS of multiple MICP-treated sand samples in one wet-dry cycle

Sand Type	Times of MICP treatment	Average UCS of unweathered samples (MPa)	Average UCS of weathered samples (MPa)	UCS loss rate (%)
Ottawa silica sand	1	1.25	0.22	82.4
	2	2.87	2.86	0.35
	3	3.58	3.21	10.33
	4	4.24	4.26	0

3.5 Durability results of MICP-treated specimens during various freeze-thaw cycles

3.5.1 Unconfined compressive strength results

The stress-strain curves at 0, 5, 10, and 15 freeze-thaw (F-T) cycles obtained from unconfined compression tests on the MICP-treated sands are shown in Figure 3-13. The unconfined compressive strengths of MICP-treated Ottawa silica sand decrease gradually when they are exposed to severe conditions (more freeze-thaw cycles). The highest strength reduction (73.7% loss) for the MICP-treated Ottawa silica sand occurred at the 15th cycle. Figure 3-13(b) shows the stress-strain relationship of UCS for MICP-treated Biloxi beach sand samples at 0, 5, 10, and 15 freeze-thaw (F-T) cycles. The peak strength of unweathered samples is about 1.33 MPa, then it dropped to 1.1 MPa after 5 cycles of F-T. After 10 and 15 F-T cycles, the peak strength of MICP-treated Biloxi beach sand samples continuously decreased to 0.88 MPa and 0.8 MPa, respectively. The behavior of MICP-treated Biloxi beach sand samples is similar to MICP-treated Ottawa sand samples in the freeze-thaw cycle.

Table 3-6 summarized that the MICP-treated Ottawa silica sand samples only had about 26% of initial strength remained after 15 freeze-thaw cycles compared with unweathered samples. For comparison, the MICP-treated Biloxi beach sand samples had better ability to resist the freeze-thaw cycles, they still had about 62% of initial strength remained after 15 freeze-thaw cycles compared with unweathered samples.

Table 3-6 UCS of MICP-treated sand in various freeze-thaw cycles

Sand Type	Average UCS of unweathered samples (MPa)	Times of freeze-thaw cycles	Average UCS of weathered samples (MPa)	UCS loss rate (%)
Ottawa silica sand	1.98	5	1.08	45.45
		10	0.65	67.17
		15	0.52	73.74
Biloxi beach sand	1.33	5	1.12	15.79
		10	0.91	31.58
		15	0.82	38.35

Box plot of UCS as a function of weathered number is shown in Figure 3-14. It can be summarized that no matter for MICP-treated Ottawa silica sand samples (Figure 3-14(a)) or MICP-treated Biloxi beach sand samples (Figure 3-14(b)), the UCS of MICP-treated specimens decreased gradually along with freeze-thaw cycles.

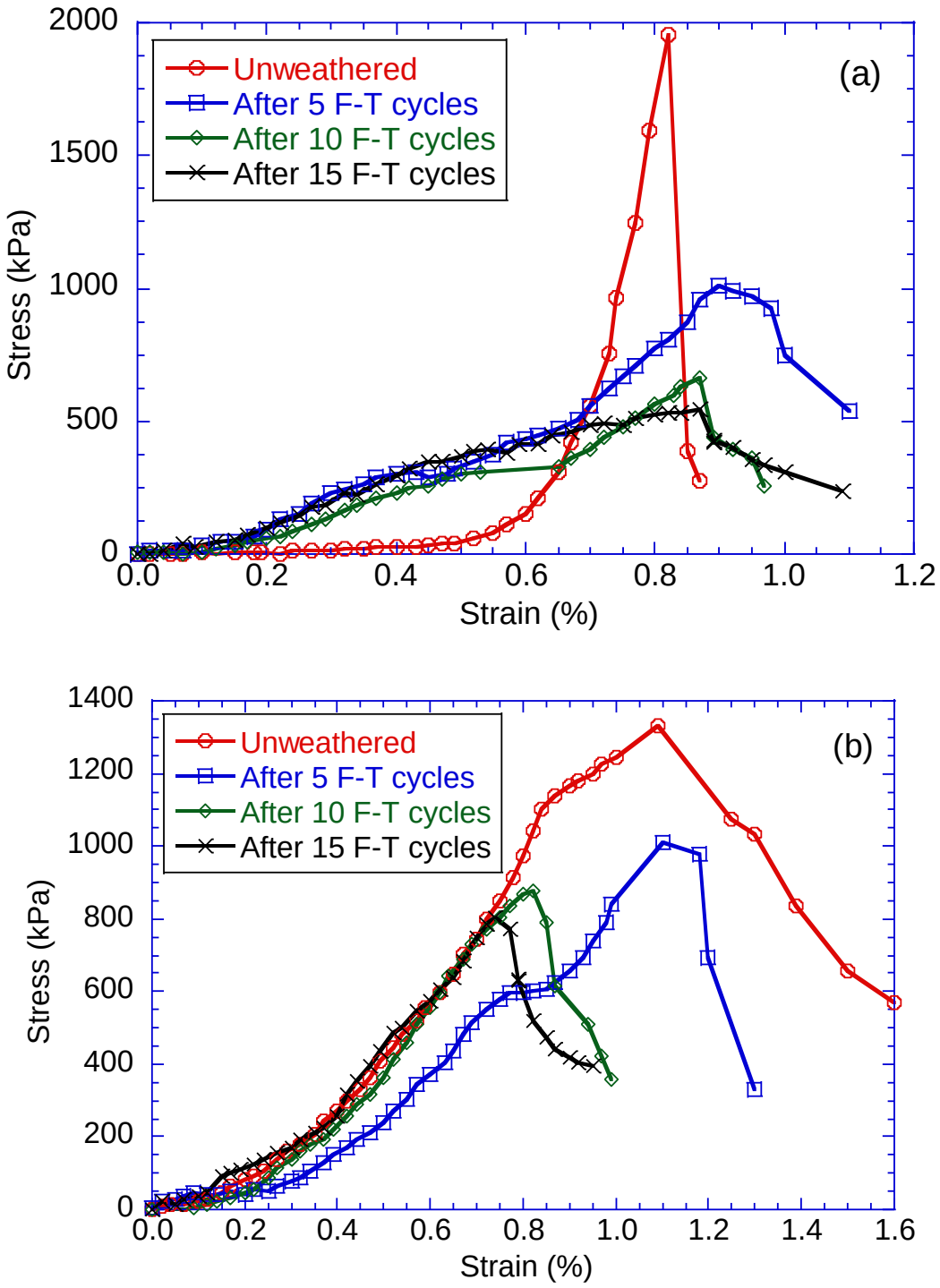

Figure 3-13 Stress-strain relationship of MICP-treated sand samples during freeze-thaw cycles (a) Ottawa silica sand; (b) Biloxi beach sand.

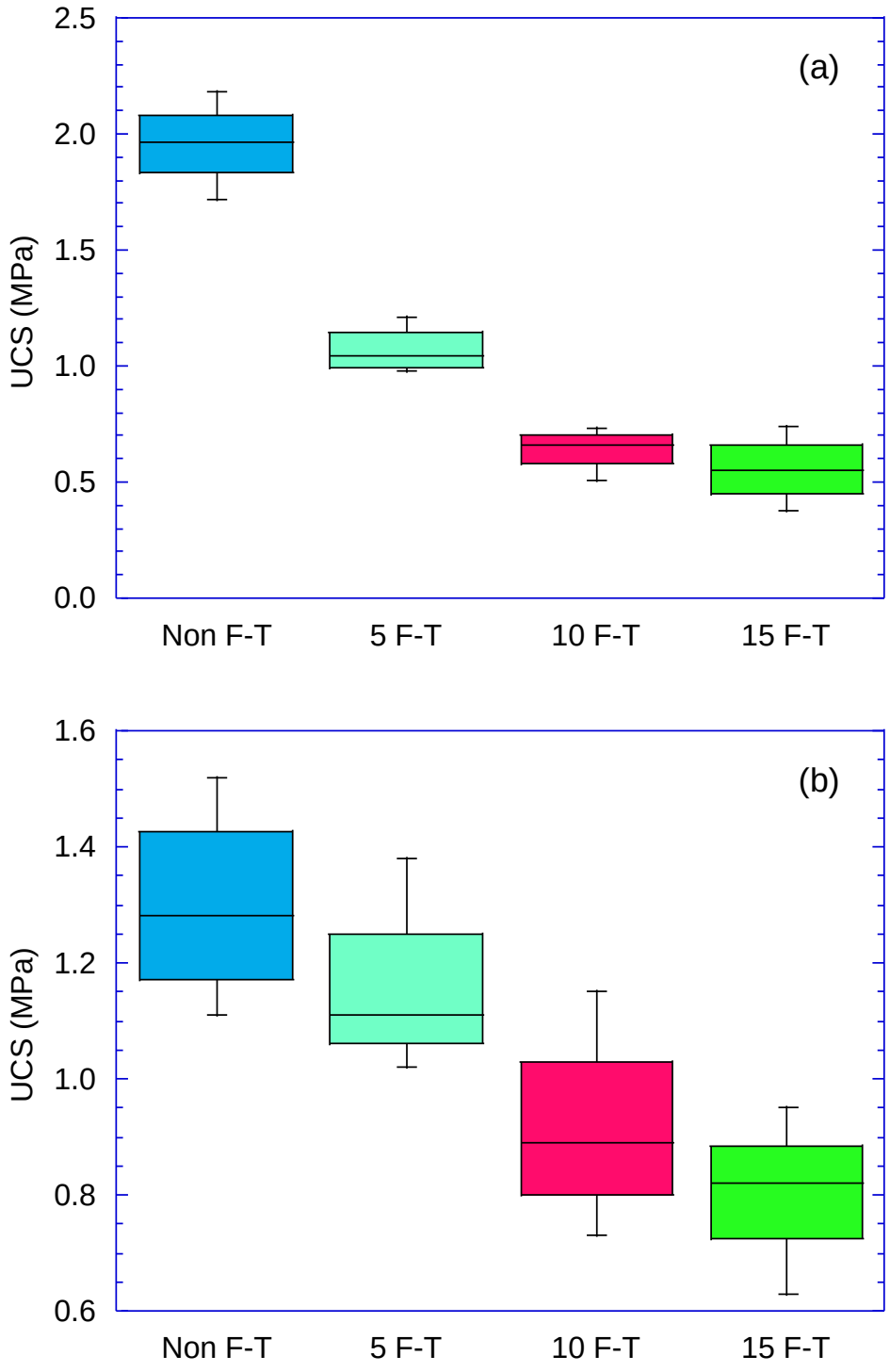

Figure 3-14 Box plot of UCS for MICP-treated sand samples as a function of weathered number (a) Ottawa silica sand; (b) Biloxi beach sand

3.5.2 Attenuation coefficient

To demonstrate the effect of the freeze-thaw cycles on MICP-treated Ottawa silica sand and MICP-treated Biloxi beach sand, freeze-thaw attenuation coefficient is introduced. The freeze-thaw attenuation coefficient (η_f) is defined as the proportion of the unconfined compressive strength (q_u) before and after the freezing and thawing treatment, which reflects the extent to which freezing and thawing affect MICP-treated sand. The freeze-thaw attenuation coefficient formula is defined as follows:

(3.2)

where, q_{ui} is the initial unconfined compressive strength of samples before applying a freeze-thaw cycle, and q_{un} is the unconfined compressive strength of samples after applying n freeze-thaw cycles.

The unconfined compressive strength attenuation coefficient results for MICP-treated Ottawa silica sand and MICP-treated Biloxi beach sand samples subjected to freeze-thaw cycles are given in Figure 3-15. As shown in this figure, the unconfined compressive strength attenuation coefficients of both these two types of MICP-treated sand samples decline significantly after the first wet-dry cycle. But the trend is more obvious for Ottawa silica sand. The unconfined compressive strength attenuation coefficients of these two types of samples decreases gradually by increasing the number of freeze-thaw cycles, declines to 0.26 for MICP-treated Ottawa silica sand samples, and decline to 0.62 for MICP-treated Biloxi beach sand samples after 15 freeze-thaw cycles. The MICP-treated Biloxi beach sand has better resistance on freeze-thaw cycles than MICP-treated Ottawa silica sand.

4. Impacts/Benefits of Implementation

This project is to address the MarTRAC mission in the area of "Multimodal Infrastructure Asset and Material Resiliency", and "Sustainable Multimodal Infrastructure". The results of this study bring an important finding that MICP-treated material was weak at wet-dry durability and freeze-thaw durability. But MICP-treated beach sand material was better at resisting these two weather conditions possibly because of its irregular shaped particles. The use of fiber or multiple treatments during the MICP treatment can provide resistance to the weathered deteriorations of MICP-treated soil. In addition, the bacteria come from natural soil so that MICP is environment-friendly. The MICP treatment establishes a cost-effective and *in situ* improvement of the engineering properties of sandy soils in coastal area for maritime transportation infrastructure construction. The use of MICP in coastal engineering brings positive impacts for the sustainable coastal infrastructure contrition materials.

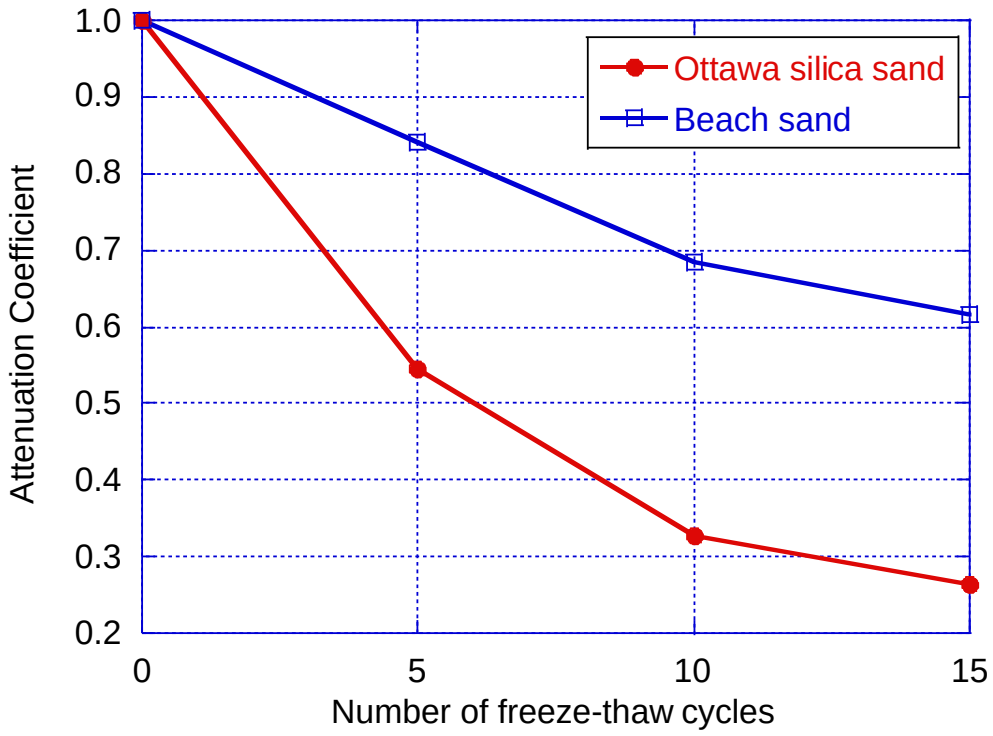

Figure 3-15 Attenuation coefficient of MICP-treated sand as a function of weathered number

5. Recommendations and Conclusions

The various factors that influence on soil properties of bio-mediated soils, including bacteria concentration, cementation media concentration, reaction time, sand type, amount of oxygen (Bundur et al. 2017, Li et al. 2017) and curing conditions have been studied with the new sample preparation mold. The results of unconfined compression test show that the experimental factors (bacteria/urease concentration, cementation media concentration, reaction time, and type of sand) have significant impact on the MICP process and engineering properties of sand treated by both bacteria and urease, while the curing conditions has small effect. The unconfined compression strength (1.76~2.04 MPa) of bacteria treated samples is almost 5 times that (0.33~0.43 MPa) of urease treated samples under similar urease activity. The MICP process catalyzed by bacteria is much more effective than the one catalyzed by urease in terms of engineering soil properties improvement (Zhao, Li et al. 2014a).

This study is to develop bio-mediated particulate materials to enhance the resilience and protection of maritime transportation infrastructure elements. The advanced materials are based on MICP for the sandy soils in the coastal area. Experimental works had been conducted to study the effect of sample preparation method, impact of bacteria concentration, impact of cementation media concentration, durability impact of wet-dry cycles, and durability impact of freeze-thaw cycles on the mechanical properties of MICP-treated Ottawa sand and MICP-treated

beach sand. The experimental results indicated that wet-dry cycles and freeze-thaw cycles could result in sharp decrease on unconfined compressive strength. But the MICP-treated beach sand samples still had about 29.8% of initial strength remained after five wet-dry cycles, and still about 60% of initial strength remained after fifteen freeze-thaw cycles compared with unweathered samples. The MICP-treated beach sand samples were better to resist wet-dry cycles and freeze-thaw cycles compared with MICP-treated Ottawa silica sand samples, which indicate that it is possible to apply MICP to coastal engineering in order to improve the strength of MICP-treated material. Two reinforced methods, including distributed fiber and multiple MICP treatment, were studied to improve the resistance of MICP-treated sandy soil on wet-dry durability. The results showed that these two reinforced methods are both significant to resist the weathered condition. The multiple MICP treatments even can resist the wet-dry cycles nearly 100%. All these results indicate that the bio-mediated particulate material based on MICP can provide an effective solution for problematic cases of sandy soil in the coastal area and beach sands. It is recommended that a pilot scale test be further performed to more closely simulate the real-life durability condition of MICP-treated soils in coastal area.

References

ASTM (2015), ASTM D559 – 15 Standard Test Methods for Wetting and Drying Compacted Soil-Cement Mixtures, Vol. 04.08

ASTM (2016), ASTM D560 – 16 Standard Test Methods for Freezing and Thawing Compacted Soil-Cement Mixtures, Vol. 04.08

ASTM (2013), ASTM D2166/D2166M – 13 Standard Test Method for Unconfined Compressive Strength of Cohesive Soil

Akiyama, M., D. M. Frangopol and M. Suzuki (2012). "Integration of the effects of airborne chlorides into reliability-based durability design of reinforced concrete structures in a marine environment." Structure and Infrastructure Engineering **8**(2): 125-134.

Bang, S. (2015). "Welcome to microbiology at South Dakota School of Mines and Technology." ⟨http://ssbang.sdsmt.edu/⟩ (Aug. 13, 2015).

Bundur, Z. B., A. Amiri, Y. C. Ersan, N. Boon and N. De Belie (2017). "Impact of air entraining admixtures on biogenic calcium carbonate precipitation and bacterial viability." Cement and Concrete Research **98**: 44-49.

Cai, H. and X. Liu (1998). "Freeze-thaw durability of concrete: ice formation process in pores." Cement and concrete research **28**(9): 1281-1287.

Chou, C.-W., E. A. Seagren, A. H. Aydilek and M. Lai (2011). "Biocalcification of sand through ureolysis." Journal of Geotechnical and Geoenvironmental Engineering **137**(12): 1179-1189.

Consoli, N. C., M. A. Vendruscolo, A. Fonini and F. Dalla Rosa (2009). "Fiber reinforcement effects on sand considering a wide cementation range." Geotextiles and Geomembranes **27**(3): 196-203.

DeJong, J. T., M. B. Fritzges and K. Nüsslein (2006). "Microbially induced cementation to control sand response to undrained shear." Journal of Geotechnical and Geoenvironmental Engineering **132**(11): 1381-1392.

Jiang, N.-J., H. Yoshioka, K. Yamamoto and K. Soga (2016). "Ureolytic activities of a urease-producing bacterium and purified urease enzyme in the anoxic condition: Implication for subseafloor sand production control by microbially induced carbonate precipitation (MICP)." Ecological Engineering **90**: 96-104.

Li, J., X. Wenyu, C. Jianguo, L. Li and G. Yushi (1999). "Stydy on the mechanism of concrete destruction under frost action." Journal of Hydraulic Engineering **1**.

Li, C., D. Yao, S. Liu, T. Zhou, S. Bai, Y. Gao and L. Li (2017). "Improvement of geomechanical properties of bio-remediated Aeolian sand." Geomicrobiology Journal (just-accepted): 00-00.

Li, M., L. Li, U. Ogbonnaya, K. Wen, A. Tian and F. Amini (2015). "Influence of fiber addition on mechanical properties of MICP-treated sand." Journal of Materials in Civil Engineering **28**(4): 04015166.

Li, M., K. Wen, Y. Li and L. Zhu (2017). "Impact of oxygen availability on microbially induced calcite precipitation (MICP) treatment." Geomicrobiology Journal: 1-8.

Mörsdorf, G. and H. Kaltwasser (1989). "Ammonium assimilation in Proteus vulgaris, Bacillus pasteurii, and Sporosarcina ureae." Archives of microbiology **152**(2): 125-131.

Mortensen, B., M. Haber, J. DeJong, L. Caslake and D. Nelson (2011). "Effects of environmental factors on microbial induced calcium carbonate precipitation." Journal of applied microbiology **111**(2): 338-349.

Pham, V. P., A. Nakano, W. R. van der Star, T. J. Heimovaara and L. A. van Paassen (2016). "Applying MICP by denitrification in soils: a process analysis." Environmental Geotechnics: 1-15.

Qabany, A. A., Soga, K., and Santamarina, C. (2012). "Factors affecting efficiency of microbially induced calcite precipitation." J. Geotech. Geoenviron. Eng. 138, 992-1001.

Shao, W., B. Cetin, Y. Li, J. Li and L. Li (2014). "Experimental investigation of mechanical properties of sands reinforced with discrete randomly distributed fiber." Geotechnical and Geological Engineering **32**(4): 901-910.

Stocks-Fischer, S., J. K. Galinat and S. S. Bang (1999). "Microbiological precipitation of $CaCO_3$." Soil Biology and Biochemistry **31**(11): 1563-1571.

Van Paassen, L. A. (2009). "Biogrout, ground improvement by microbial induced carbonate precipitation." Doctoral Thesis, TUDelft.

Whiffin, V. S. (2004). Microbial $CaCO_3$ precipitation for the production of biocement, Murdoch University.

Whiffin, V. S., L. A. van Paassen and M. P. Harkes (2007). "Microbial carbonate precipitation as a soil improvement technique." Geomicrobiology Journal **24**(5): 417-423.

Zhao, Q., L. Li, C. Li, M. Li, F. Amini and H. Zhang (2014a). "Factors affecting improvement of engineering properties of MICP-treated soil catalyzed by bacteria and urease." Journal of Materials in Civil Engineering **26**(12): 04014094.

Zhao, Q., L. Li, C. Li, H. Zhang and F. Amini (2014b). "A full contact flexible mold for preparing samples based on microbial-induced calcite precipitation technology."